

Role of the Heat Sink Layer Ta for Ultrafast Spin Dynamic Process in Amorphous TbFeCo Thin Films

Y. Ren^{*,§}, Z. Z. Zhang[†], T. Min^{‡,¶} and Q. Y. Jin[†]

**School of Physics and Astronomy
Yunnan University, Kunming 650091
Yunnan, P. R. China*

*†Department of Optical Science and Engineering
Fudan University, Shanghai 200433, P. R. China*

*‡State Key Laboratory for Mechanical Behavior of Materials
Xi'an Jiaotong University
Xi'an 710049, Shanxi, P. R. China
§reny@lzu.edu.cn
¶tai.min@xjtu.edu.cn*

Received 16 March 2017

Accepted 5 April 2017

Published 15 May 2017

The ultrafast demagnetization processes (UDP) in Ta (t nm)/TbFeCo (20 nm) films have been studied using the time-resolved magneto-optical Kerr effect (TRMOKE). With a fixed pump fluence of 2 mJ/cm^2 , for the sample without a Ta underlayer ($t = 0$ nm), we observed the UDP showing a two-step decay behavior, with a relatively longer decay time (τ_2) around 3.0 ps in the second step due to the equilibrium of spin-lattice relaxation following the $4f$ occupation. As a 10 nm Ta layer is deposited, the two-step demagnetization still exists while τ_2 decreases to $\sim 1.9 \text{ ps}$. Nevertheless, the second-step decay ($\tau_2 = 0 \text{ ps}$) disappears as the Ta layer thickness is increased up to 20 nm, only the first-step UDP occurs within 500 fs , followed by a fast recovery process. The rapid magnetization recovery rate strongly depends on the pump fluence. We infer that the Ta layer provides conduction electrons involving the thermal equilibrium of spin-lattice interaction and serves as heat bath taking away energy from spins of TbFeCo alloy film in UDP.

Keywords: Ultrafast spin dynamics; heat sink layer; TbFeCo films; TRMOKE.

1. Introduction

Laser-induced ultrafast spin dynamics processes explored by time-resolved magneto-optical Kerr effect (TRMOKE) have received considerable attention in the last decades.^{1–4} On the one hand, for basic research, the characteristic time of excitation

and relaxation for a magnetic system could be directly obtained in ultrafast demagnetization and recovery processes by TRMOKE. On the other hand, a crucial issue of magnetic recording with the ever-growing recording density is to improve the speed of reading and writing data-storage

[§]Corresponding author.

information, and the speed limit of data storage could be explored by TRMOKE.

Usually, the ultrafast demagnetization process (UDP) in 3d transition metals (TM) is finished within a sub-picosecond time scale, which is usually accompanied by a recovery process in several picoseconds (*ps*) ascribed to highly efficient spin-lattice relaxation.^{5–10} However, for the rare-earth (RE)-doped TM thin films (RE-TM), the UDP may include two parts, a transient sharp demagnetization process completed within a sub-*ps* time scale (τ_1) and a relatively slow demagnetization process (longer decay τ_2) ranging from several *ps* to tens of *ps*.^{11–18} Various factors including materials,^{11,15,16} dual-pump manipulation,¹⁷ pump fluences,¹⁸ etc were studied to understand the mechanism of the UDP for the RE-TM alloy thin films. The long decay τ_2 of the second demagnetization step could be ascribed to the equilibrium of spin-lattice coupling following the 4*f* occupation as reported.¹⁴ However, how to modulate the decay time τ_2 is still not clear. Considering the great potential applications of RE-TM thin films for all-optical switching, it is essential to clarify and improve the efficiency of demagnetization process.

The dynamic demagnetization and recovery processes for magnetic films depend on the energy transfer among electrons, lattices, and spins, and on the lateral heat propagation between the laser spot and its surroundings. In particular, the cooling rate of magnetic layer strongly depends on the capability of the heat transfer between the magnetic layer and the heat sink layer. It was reported that the recovery rate of ultrafast demagnetization for 3d-TM films is strongly related to the material and thickness of heat sink layers.^{19–22} However, research work focusing on the effects of heat sink layers on the UDP of the RE-TM thin films are still very limited. Therefore, in this work, we performed a detailed study on the UDP for TbFeCo films with a Ta heat sink layer, trying to get a general insight into the mechanism of spin-flip processes mediated by hot electrons via heat sink layer.

The ultrafast demagnetization and corresponding recovery processes of Ta (*t* nm)/Tb_{0.18}(Fe_{0.88}Co_{0.12})_{0.82}(20 nm) with various *t* were systematically studied by TRMOKE. We observed that the critical slow demagnetization time and recovery time are strongly related to the pump fluence, the substrate temperature, and thickness of the Ta heat sink layer.

2. Experiments

A series of Si/Ta (*t* nm)/Tb_{0.18}(Fe_{0.88}Co_{0.12})_{0.82}(= TbFeCo) (20 nm) and Fe_{0.88}Co_{0.12} (20 nm) (= FeCo) samples were fabricated by DC magnetron sputtering with different Ta layer thicknesses. The base pressure of the chamber was 5×10^{-8} Torr and the Ar working pressure was 5 mTorr. 4-nm thick Ta capping layers were used in all samples to prevent the samples from oxidation. The composition of TbFeCo was controlled by modifying the deposition power of each individual target and measured by X-ray photoemission spectra. The microstructure of samples was analyzed by X-ray diffraction (XRD) as shown in Fig. 1. The TbFeCo layers in all the samples were amorphous, but the Ta layers of 10 nm and 20 nm thick were in a polycrystalline state. The UDP was measured by TRMOKE at various temperatures in the longitudinal geometry, with applying a saturated in-plane magnetic field of ± 2.0 kOe. The easy magnetization direction of all samples was in the film plane. Details of the fabrication and TRMOKE measurements can be seen elsewhere.¹⁸ The TbFeCo film has a Curie Temperature (T_c) of 400 K measured by physical property measurement system (PPMS).

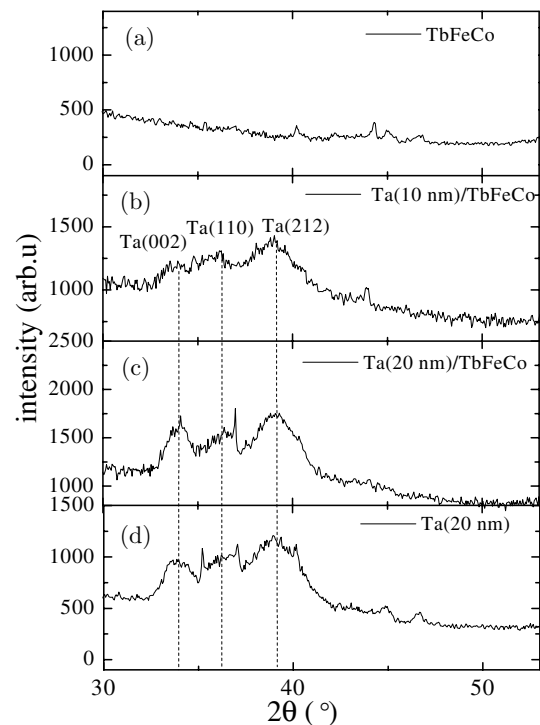


Fig. 1. X-ray scan of Ta(*t* nm)/TbFeCo (20 nm) films for *t* = 0 nm (a), *t* = 10 nm (b), *t* = 20 nm (c) and (d) Ta (20 nm) thin film samples.

3. Results and Analysis

Figure 2(a) shows the typical time resolved magneto-optical Kerr signals of the TbFeCo film versus delay time measured at various substrate temperatures (T). For these measurements, the pump fluence is fixed as $p = 2.0 \text{ mJ/cm}^2$. At 300 K, a two-step UDP is observed, the second slow demagnetization process occurs within a time scale of 1–6 ps after the first conventional fast stage. It suggests that the spin-lattice equilibrium might be delayed by following the $4f$ occupation of Tb, whose orbital moments reside in the f -shell.^{12,14} By increasing T from 300 K to 380 K, the amplitude of demagnetization reduces, while the second slow decay step gradually decreases and even disappears. At 380 K (below the T_c of the TbFeCo film), the previous slow magnetization decay is nearly replaced by a slow recovery process within the timescale of several ps. In order to evaluate the impact of substrate temperature on the characteristic time for magnetization demagnetization process, we propose to analyze the results by using a bi-exponential function to fit the dynamic magnetization behavior after laser excitation. The function has a form of

$A(t)/A(0) = A_1 \times \exp(-t/\tau_1) + A_2 \times \exp(-t/\tau_2) + C$, where A_1 , A_2 , τ_1 and τ_2 are the amplitudes and lifetimes of the first fast and the second slow demagnetization processes, respectively, and C is a constant. Figure 2(b) shows the dependences of τ_1 and τ_2 on various T . It is found that τ_1 is basically a constant of $\sim 500 \text{ fs}$, which is related to the intrinsic spin-flipping characteristic of CoFe. However, τ_2 decreases obviously from $3.01 \pm 0.045 \text{ ps}$ to $0.6 \pm 0.023 \text{ ps}$ as T increases from 300 K to 370 K, and finally decreases down to 0 ps at 380 K, which should be related to Tb atoms due to its low T_c . Figure 2(c) shows the dependence of A_1 and A_2 versus substrate temperatures. A_1 drastically decreases from 0.70 ± 0.03 to 0.25 ± 0.03 and A_2 slightly reduces from 0.19 ± 0.04 to 0 with raising T from 300 K to 380 K, respectively. A possible explanation for the results is below. Since the spin ordering in the magnetic ordering state has been already disturbed by increasing T without laser heating, the impulsion of pump beam will give rise to a reduced demagnetization amplitude for the samples with higher T . Moreover, in the TbFeCo system, the $4f$ spins of Tb could become a more disordered paramagnetic state by increasing T , since the FeCo alloy has a much higher Curie temperature than the Tb ($T_c \sim 219.5 \text{ K}$ for Tb, 1043 K for Fe, and 1403 K for Co). The less $4f$ electrons participate in the UDP, the faster spin-lattice equilibrium takes place, resulting in decreasing τ_2 with increasing T . It further suggests that the second long demagnetization process of TbFeCo is dominated by the $4f$ electrons of Tb.

To improve the possibility of heat transfer from the $4f$ electrons to the conduction band, the transient demagnetization processes were measured at 300 K for TbFeCo films with different Ta layer thicknesses. Figure 3(a) shows the typical TRMOKE signals of Ta ($t \text{ nm}$)/ TbFeCo and a pure FeCo film measured under $p = 2.0 \text{ mJ/cm}^2$. Apparently, for the TbFeCo film with $t = 10 \text{ nm}$, the two-step decay of the UDP still exists. However, for both the TbFeCo film with a 20 nm thick Ta underlayer and the pure FeCo film without a Ta underlayer, the UDP is accomplished within one ps, leaving only the first fast stage. No second-step demagnetization is found, a rapid recovery process of several ps occurs immediately after the first demagnetization step. The one-step fast demagnetization time τ_1 could be fitted by the equation as described elsewhere.²¹ To analyze the results in quantity, A_1 , A_2 , τ_1 and τ_2 are

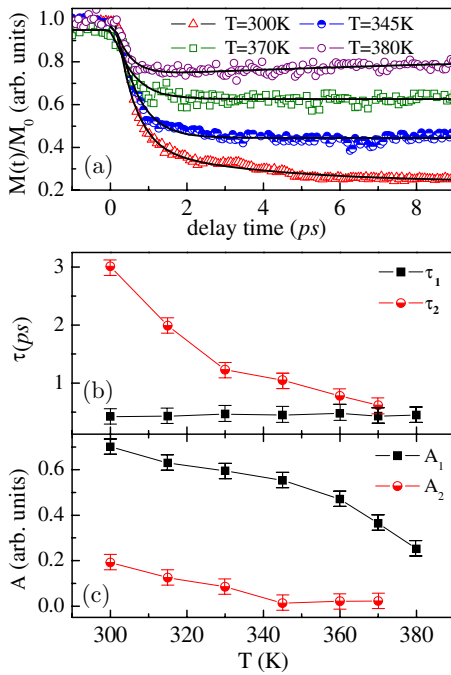


Fig. 2. (a) Time-resolved transient Kerr signal of TbFeCo (20 nm) films for pump fluences of 2.0 mJ/cm^2 with substrate temperature (T) ranging from 300 to 380 K. Corresponding τ_1 , τ_2 (b), A_1 and A_2 (c) for various T extracted from TRMOKE measurements with systematic error bars.

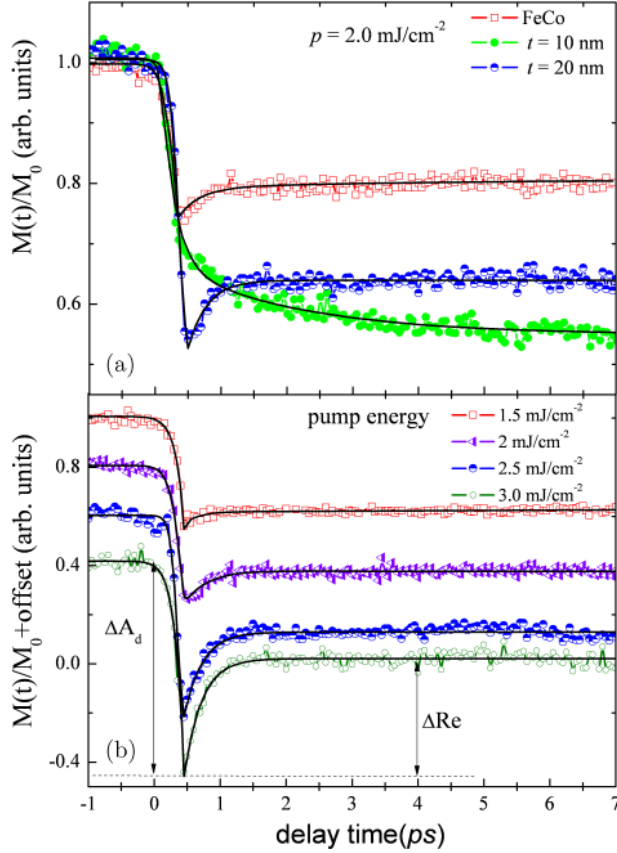


Fig. 3. Transient Kerr signals of (a) Ta (t nm)/TbFeCo (20 nm) and FeCo (20 nm) films for pump fluences of 2.0 mJ/cm² and (b) Ta (20 nm)/TbFeCo (20 nm) for pump fluences of 1.5, 2.0, 2.5, 3.0 in the unit of mJ/cm² from top to bottom.

fitted and shown in Table 1. For all the samples, τ_1 corresponds to the fast demagnetization process, which is generally smaller than 500 fs for all the films due to bleaching effect.² In contrast, τ_2 decreases from 3.01 ± 0.45 ps to 0 (without second slow stage) with t increasing from 0 to 20 nm. Note that A_1 is 0.26 ± 0.03 for FeCo film, while it is 0.46 ± 0.03 for Ta (20 nm)/TbFeCo film, which could be explained by the lower T_c for the latter case. Moreover, we find that the total amplitude of demagnetization ($A_1 + A_2$) decreases as Ta layer thickness increases

from 0 to 20 nm, suggesting that the magnetic disorder induced by laser pumping reduces due to the enhanced heat sink effect.

To deeply understand the mechanism of the one-step demagnetization process for TbFeCo film with a 20 nm thick Ta underlay, the transient Kerr signals as a function of delay time for pump fluence varying from 1.5 to 3.0 mJ/cm² for Ta (20 nm)/TbFeCo film are shown in Fig. 3(b). For all the pump fluences, the ultrafast demagnetization is accomplished within about 500 fs. For each sample, the maximum reduction amplitude ΔA_d of transient magnetization increases with increasing the pump fluence. As we know, the more the hotter electrons are induced by fs laser, the less order of spin maintains, resulting in a larger ΔA_d . As the delay time is longer than 4.0 ps, the transient magnetization increases much slowly in the recovery process, depending on the heat transfer rate from spins to the surroundings. We defined the recovery amplitude ΔRe at time delay of 4.0 ps. For Ta (20 nm)/TbFeCo film, we observed that the magnetization recovery rate $\Delta Re / \Delta A_d$ increases with increasing p . The $\Delta Re / \Delta A_d$ in delay time of 4.0 ps amounts to about 17.6%, 21.3%, 41.2% and 53.7% for $p = 1.5, 2.0, 2.5$ and 3.0 mJ/cm², respectively. It suggests that the energy transfers efficiently from TbFeCo layer to the heat sink Ta layer for higher pump fluences.

A phenomenological theory is provided as follows. The demagnetization process in TbFeCo alloy films is dominated by both 3d electrons and 4f electrons which are coupled through the conduction electrons. For a strong coupling between 4f and 3d spins, the effect of 4f shell on the thermal equilibrium will delay the demagnetization process. By increasing the thickness of Ta layer, conduction electrons (energy transfer channels) increase, which will interact with 4f spins and then take away the energy from 4f spins to the heat bath via the lattice of Ta layer. As a result, for $t = 20$ nm, the second slow demagnetization process disappears and the

Table 1. This Parameters for Ta (t nm)/TbFeCo (20 nm) and FeCo (20 nm) thin films extracted from TRMOKE measurements.

Films	τ_1 (ps)	τ_2 (ps)	A1 (arb. units)	A2 (arb. units)
FeCo	0.40 ± 0.03	0	0.26 ± 0.03	N/A
TbFeCo	0.42 ± 0.02	3.01 ± 0.45	0.70 ± 0.03	0.19 ± 0.04
Ta (10nm)/TbFeCo	0.41 ± 0.03	1.92 ± 0.22	0.36 ± 0.04	0.12 ± 0.02
Ta (20 nm)/TbFeCo	0.42 ± 0.02	0	0.46 ± 0.03	N/A

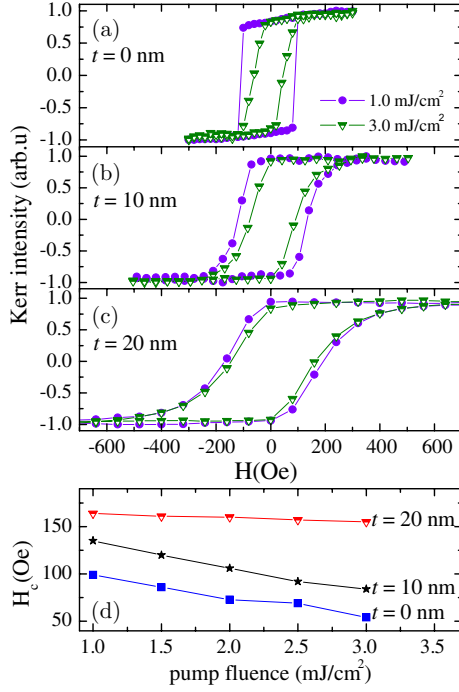


Fig. 4. Transient Kerr loops of Ta (t nm)/TbFeCo (20 nm) films for pump fluences of 1.0 and 3.0 mJ/cm^2 for $t = 0$ nm (a), $t = 10$ nm (b) and $t = 20$ nm (c), respectively. (d) The coercivity H_c extracted from Kerr loops as a function of pump fluence for Ta (t nm)/TbFeCo (20 nm) films.

amplitude of demagnetization drastically reduces, accompanied by a rapid recovery process.

Above analysis can be further confirmed by more experimental evidences. The transient Kerr loops for TbFeCo films with and without the Ta heat sink layer were measured at a delay time of 4.0 ps and at $T = 300$ K, as shown in Figs. 4(a)–4(c). For all the samples here, the switching field H_s and coercivity H_c decrease with increasing p from 1.0 to 3.0 mJ/cm^2 , respectively, which could be ascribed to the laser-induced heating effect. For $t = 0$ nm, the Kerr loop shows a good squareness at $p = 1.0$ mJ/cm^2 . However, it becomes tilted as increasing p to 3.0 mJ/cm^2 . It suggests that magnetic anisotropy and spin ordering of TbFeCo film are changed by pump fluence. As t increases from 10 to 20 nm, the coercivity H_c increases for a fixed pump fluence, and then a long ‘tail’ is observed in all the Kerr loops with various pump fluence. The H_c dependence on the pump fluence is summarized in Fig. 4(d). For $t = 0$ nm, the H_c decreases considerably from 99 Oe to 54 Oe (declines nearly 46%) with p increasing from 1.0 to 3.0 mJ/cm^2 . With the increase of t , the H_c reduction becomes gradual. As seen for

$t = 20$ nm, the H_c decreases only a little bit, from 164 Oe to 155 Oe (declines 5.5%). It infers that magnetic anisotropy is enhanced by adding a Ta layer, and the magnetic properties are less affected by pump fluences for the TbFeCo films with a thick Ta layer. The heat energy induced by pump beam easily transfers from the 3d and 4f electrons to the heat bath provided by the thick Ta layer, leading to a fast recovery of magnetization in the TbFeCo layer. Moreover, the increased magnetic anisotropy enhances the ability of spins of TbFeCo to resist thermal disturbance.

In summary, the UDP of Ta (t nm)/TbFeCo films were systematically studied by varying substrate temperature T , the Ta underlayer thickness t and the pump fluence. We observed a two-step demagnetization process for TbFeCo films without Ta layer or with a thin Ta layer. The second slow demagnetization process gradually disappears with increasing T or t , suggesting the second slow demagnetization is related to the 4f electrons of Tb. For $t = 20$ nm, the UDP is accomplished by one step within about 500 fs and followed by a fast magnetization recovery within several ps . It suggests that conduction electrons increase with increasing Ta layer thickness, which will interact with 4f spins and take away the energy from 4f spins, leading to the second-step magnetization decay replaced by a fast recovery. Meanwhile, the magnetic anisotropy could be enhanced by increasing t , which might enhance resistance to the laser-induced heating effect. This allows designing magnetic devices using a proper heat sink layers to improve possible recording speed in RE-TM alloy thin films.

Acknowledgments

This work is supported by the National Natural Science Foundation of China (Grant Nos. 51201081, 61366002, 61664009, 11674142 and 61465015), Research Funds for the Central Universities (Grant No. lzujbky-2016-124), Research Funds for East-land young teachers training program of Yunnan University, and the High-end Scientific and Technological Talents Introduction Project of Yunnan Province (Grant No. 2013HA019).

References

1. E. Beaurepaire, J. C. Merle, A. Daunois and J. Y. Bigot, *Phys. Rev. Lett.* **76**, 4250 (1996).

2. B. Koopmans, M. van Kampen, J. T. Kohlhepp and W. J. M. de Jonge, *Phys. Rev. Lett.* **85**, 844 (2000).
3. W. He, H. Y. Wu, J. W. Cai, Y. W. Liu and Z. H. Cheng, *Spin* **5**, 1540014 (2015).
4. X. Jiao, Z. Z. Zhang and Y. W. Liu, *Spin* **6**, 1650003 (2016).
5. U. Conrad, J. Güdde, V. Jähnke and E. Matthias, *Appl. Phys. B.* **68**, 511 (1999).
6. J. Y. Bigot, L. Guidoni, E. Beaurepaire and P. N. Saeta, *Phys. Rev. Lett.* **93**, 077401 (2004).
7. B. Koopmans, J. J. M. Ruigrok, F. Dalla Longa and W. J. M. de Jonge, *Phys. Rev. Lett.* **95**, 267207 (2005).
8. J. Y. Bigot, M. Vomir, L. H. F. Andrade and E. Beaurepaire, *Chem. Phys.* **318**, 137 (2005).
9. T. Kampfrath, R. G. Ulbrich, F. Leuenberger, M. Münzenberg, B. Sass and W. Felsch, *Phys. Rev. B.* **65**, 104429 (2001).
10. I. Radu, C. Stamm, A. Eschenlohr, F. Radu, R. Abrudan, K. Vahaplar, T. Kachel, N. Pontius, R. Mitzner, K. Holldack, A. Föhlich, T. A. Ostler, J. H. Mentink, R. F. L. Evans, R. W. Chantrell, A. Tsukamoto, A. Itoh, A. Kirilyuk, A. V. Kimel and T. Rasing, *Spin* **5**, 1550004 (2015).
11. M. Lisowski, P. A. Loukakos, A. Melnikov, I. Radu, L. Ungureanu, M. Wolf and U. Bovensiepen, *Phys. Rev. Lett.* **95**, 137402 (2005).
12. I. Radu, G. Woltersdorf, M. Kiessling, A. Melnikov, U. Bovensiepen, J. U. Thiele, and C. H. Back, *Phys. Rev. Lett.* **102**, 117201 (2009).
13. B. Koopmans, G. Malinowski, F. Dalla Longa, D. Steiauf, M. Fahnle, T. Roth, M. Cinchetti and M. Aeschlimann, *Nat. Mater.* **9**, 259 (2010).
14. M. Wietstruk, A. Melnikov, C. Stamm, T. Kachel, N. Pontius, M. Sultan, C. Gah, M. Weinelt, H. A. Dürr and U. Bovensiepen, *Phys. Rev. Lett.* **106**, 127401 (2011).
15. L. Rettig, C. Dornes, N. Thielemann-Kühn, N. Pontius, H. Zabel, O. L. Schlagel, T. A. Lograsso, M. Chollet, A. Robert, M. Sikorski, S. Song, J. M. Glowia, C. Schüßler-Langeheine, S. L. Johnson and U. Staub, *Phys. Rev. Lett.* **116**, 257202 (2016).
16. D. Afanasiev, B. A. Ivanov, A. Kirilyuk, T. H. Rasing, R. V. Pisarev and A. V. Kimel, *Phys. Rev. Lett.* **116**, 097401 (2016).
17. T. Cheng, J. Wu, T. Liu, X. Zou, J. Cai, R. W. Chantrell and Y. Xu, *Phys. Rev. B* **93**, 064401 (2016).
18. Y. Ren, Y. L. Zuo, Z. Z. Zhang, Q. Y. Jin and S. M. Zhou, *IEEE Trans. Magn.* **49**, 3159 (2013).
19. C. D. Stanciu, A. V. Kimel, F. Hansteenl, A. Tsukamoto, A. Itoh, A. Kirilyuk and T. H. Rasing, *Phys. Rev. B*, **73**, 220402 (2006).
20. J. Hohlfeld, T. H. Gerrits, M. Bilderbeek, T. H. Rasing, H. Awano and N. Ohta, *Phys. Rev. B.*, **65**, 012413 (2001).
21. Y. Ren, J. Q. Zhao, Z. Z. Zhang, Q. Y. Jin, H. N. Hu and S. M. Zhou, *J. Phys. D: Appl. Phys.* **41**, 085005 (2008).
22. M. H. Tang, S. H. Chen, X. L. Zhang, Z. Z. Zhang and Q. Y. Jin, *Spin* **6**, 1650009 (2016).